BMC Pediatrics

RESEARCH

Open Access

Identification and functional analysis of *NPR2* truncating mutations in two Chinese families with short stature

Shuoshuo Wei[1,2], Rong Li[1,3], Dongye He[1,2], Chuanpeng Zhang[2], Mei Zhang[1,3], Yanying Li[1,3], Shuxiong Chen[1,2], Fupeng Liu[1,3], Bo Ban[1,2,3*†] and Qianqian Zhao[1,2*†]

Abstract

Background The signaling pathway of C-type natriuretic peptide (CNP) and its receptor (natriuretic peptide receptor 2, NPR2) is implicated in the process of endochondral ossification, which is crucial for the linear growth of long bones. Loss-of-function mutations in the NPR2 gene cause short stature. This study aimed to identify and characterize truncating mutations in NPR2 among Chinese families with short stature.

Methods Whole-exome sequencing and Sanger sequencing were conducted to identify potential mutations. Bioinformatic analysis was utilized to assess the pathogenicity of two mutations. The effects of candidate mutation on gene expression, subcellular localization, protein stability, and protein function were further assessed through in vitro assays.

Results In this study, A novel mutation, c.2629_2630delAG, p.S877Hfs*10 and a previously reported mutation, c.1162 C > T, p.R388* (ClinVar database) in NPR2, were identified in the individuals, and these variants were inherited from the mother and father, respectively. Both mutations were predicted to be deleterious and have a significant impact on protein structure based on bioinformatics analysis. In vitro experiments demonstrated that mutant mRNAs evaded nonsense-mediated mRNA decay (NMD) to produce truncated NPR2 proteins with reduced stability and increased degradation. Furthermore, two truncated NPR2 proteins exhibited impaired localization at the cell membrane and severely reduced ability to stimulate cyclic guanosine monophosphate (cGMP) production in HEK293T cells compared to wild-type (WT) NPR2 ($p < 0.05$).

Conclusion Our study identified two loss-of-function mutations of the NPR2 gene in two Chinese families and offered new insights on the pathogenesis of short stature caused by NPR2 truncating mutations.

Keywords Short stature, NPR2 gene, Truncating mutations, Truncated proteins, Loss-of-function

†Bo Ban and Qianqian Zhao contributed equally to this work and share corresponding authorship.

*Correspondence:
Bo Ban
banbo2011@163.com
Qianqian Zhao
zhaoqian930915@163.com

[1]Department of Endocrinology, Genetics and Metabolism, Affiliated Hospital of Jining Medical University, 89 Guhuai Road, Jining, Shandong 272029, P.R. China
[2]Medical Research Center, Affiliated Hospital of Jining Medical University, Jining, P.R. China
[3]Chinese Research Center for Behavior Medicine in Growth and Development, Jining, P.R. China

Introduction

Short stature (SS) is defined as a height that is at least two standard deviations (SD) below the mean for a specific population after adjusting for age and gender [1]. Approximately 80% of the variation in human height is explained by heritable factors and relatively rare single-gene mutations are involved with larger effects on stature [2, 3]. With the advancement of genetic testing technology, more and more genetic mutations associated with short stature have been detected. In a large short stature cohort, 361 mutations distributed across 111 genes were identified in 814 patients through next-generation sequencing (NGS) [4]. Moreover, in another similar study, 135 single-gene mutations were found in 561 patients with short stature by exome sequencing (ES) [5]. These mutated genes mainly affect four principal physiological processes related to short stature, namely endochondral ossification-related signaling pathways, including hormonal signaling, paracrine signaling, regulation of the cartilage extracellular matrix, and essential cellular processes [6]. The natriuretic peptide receptor 2 (NPR2) is a key player in the paracrine signaling pathway, and mutations in NPR2 significantly impact stature.

The *NPR2* gene is located at 9p13.3, including 22 exons, with a total length of approximately 16.5 kb and a full mRNA length of about 3000 bp. The NPR2, encoded by the *NPR2* gene, acts as a transmembrane guanylyl cyclases and comprises four essential domains: an extracellular ligand-binding domain (ECD), a transmembrane domain, an intracellular kinase homology domain (KHD), and a guanylyl cyclase (GC) domain [7]. Physiologically active NPR2 exists as a homodimer that increases the expression of cyclic guanosine monophosphate (cGMP) upon binding to its ligand, C-type natriuretic peptide (CNP). The CNP/NPR2/cGMP signaling pathway plays a crucial role in the proliferation and differentiation of chondrocytes, thereby facilitating the endochondral ossification process, which is accountable for the longitudinal growth in limbs and vertebrae [8, 9]. Takehito et al. demonstrated that NPR2 gene mouse knockout displays decreased body size, reduced chondrocyte population, and diminished chondrocyte proliferation activity [10]. In humans, biallelic loss-of-function mutations in the NPR2 gene result in a skeletal dysplasia known as acromesomelic dysplasia type Maroteaux (AMDM), which is characterized by extremely short and disproportionate stature [11]. In contrast, heterozygous mutations in the NPR2 gene lead to a milder phenotype, manifesting as progressive short stature with a gradual reduction in height potential over time [12]. The mechanism by which *NPR2* mutations result in short stature is not entirely clear [13]. Some short stature associated *NPR2* mutations may result in abnormal protein trafficking to the cell membrane, reduced CNP binding affinity for receptors, or inhibition of NPR2 activity [9]. However, these few studies have almost exclusively focussed on *NPR2* missense mutation and very few have investigated truncating mutations of *NPR2*.

This study identified two heterozygous truncating mutations (c.1162 C > T, p.R388* and c.2629_2630delAG, p.S877Hfs*10) in the *NPR2* gene within two families through whole exome sequencing (WES). To further understand the pathogenesis of short stature caused by *NPR2* truncating mutations, the bioinformatics analysis and in vitro functional approaches were performed to investigate the impact of truncating mutations on the expression, stability, subcellular localization and function of NPR2 protein.

Patients and methods

Patients

The patients, who originated from the Department of Endocrinology, Genetics and Metabolism at the Affiliated Hospital of Jining Medical University, sought medical attention because of their short stature. The Affiliated Hospital of Economics and Medical Sciences Ethics Committee approved the study. Written informed consent was obtained from all participants or their guardians.

Clinical evaluations

Clinical evaluation encompassed anthropometric, laboratory, and imaging assessments. Height and weight were precisely measured using a stadiometer (± 0.1 cm) and an electronic scale (± 0.1 kg). Height and weight SDS were derived from standard Chinese children's data [14]. Body mass index (BMI) was calculated as weight in kilograms divided by the square of height in meters. Genetic target height was calculated as follows: genetic target height = (paternal height + maternal height)/2 + 6.5 cm [15]. Peak growth hormone (GH) was identified through levodopa and insulin hypoglycemic tests. Serum GH was quantified by chemiluminescence (Beckman Coulter, USA; sensitivity: 0.010 μg/L). IGF-1 levels, determined by chemiluminescence immunoassay (SIEMENS, Germany; CVs: 3.0% internal, 6.2% external), were normalized to SDS based on healthy peers' data [16]. Bone age (BA) was assessed using the Greulich-Pyle (GP) method on non-dominant hand X-rays [17].

Genetic testing

Two milliliters of peripheral blood were collected from the patient and other family members, and genomic DNA was extracted using the Blood DNA Midi Kit (D3494-04, Omega BioTek, GA, USA). Whole exome sequencing (WES) was conducted with AgilentSureSelect V6 for coding exonic sequence enrichment (Agilent Technologies, CA, USA), followed by sequencing on BGISEQ-500 (BGI, Shenzhen, China) achieving 100 ×

coverage via paired-end sequencing. Post-sequencing, clean reads were aligned to the GRCh37/hg19 genome assembly using BWA (v0.7.15). Variant calling identified SNPs and InDels via GATK's HaplotypeCaller (v3.7), with data annotated using ANNOVAR. Target bases had a median coverage of 147x, with 99% ≥10x. Rare non-synonymous variants were selected, excluding common polymorphisms with MAF ≥ 0.1% in populations, referencing 1000 Genomes Project, gnomAD, and ExAC. Mutations' pathogenicity was classified per ACMG-AMP guidelines [18].

Bioinformatic analysis

Multiple sequence alignment was performed to confirm the conservation of mutated amino acid residues. The schematic diagram of the NPR2 protein structure was constructed using Adobe Illustrator (AI) to understand the mutations' location, and the approximate mutation site was identified in red. Furthermore, three-dimensional (3D) modeling of wild-type (WT) and mutant NPR2 proteins was achieved from the AlphaFold Protein Structure Database (https://alphafold.ebi.ac.uk/), and PyMOL Viewer was used to visualize the effect of the mutation on the spatial configuration of the NPR2 protein.

Construction of NPR2 lentivirus

WT and mutant NPR2-overexpression lentivirus and empty vector (EV) lentivirus were obtained from Shanghai GeneChem Co., Ltd. The human WT and mutant NPR2 gene sequences were inserted into the GV208-Flag expression vector. The vector carries the Green fluorescent protein (GFP) gene for visualization and the puromycin resistance gene for selection. The constructs were transfected into the HEK293T packaging cells to produce NPR2 lentivirus.

Transfection and generation of stable cell lines

HEK293T cell line was obtained from Shanghai Chinese Academy of Sciences cell bank (Shanghai, China). The cells were cultured in high-glucose DMEM (Gibco, USA) with 10% FBS (ExCell, China) at 37 °C in a humidified atmosphere containing 5% CO2. Before transfection, the cells were seeded in six-well plates and transfected with empty vector and NPR2 (WT and mutant) lentivirus at a MOI = 5 when they reached approximately 60-80% confluency. Empty vector lentivirus was used as a negative control for the experiments. Transfection was performed using HitransG P (GeneChem, China) as recommended. After 8 h, the transfection medium was replaced with a complete medium. Stable cell lines were generated by selecting all stable cells using puromycin (MCE, USA) at a final concentration of 5 μg/mL after 48 h.

RNA extraction and quantitative real-time PCR (qPCR) analyses

Total RNA was isolated using TRIzol (Ambion, USA), and then subjected to reverse transcription to generate cDNA employing HiScript III RT SuperMix for qPCR (Vazyme, China). Quantitative PCRs were prepared with Taq Pro Universal SYBR qPCR Master Mix (Vazyme, China) and performed on an ABI QuantStudio5 Q5 detection system. Relative mRNA expression levels were quantified by the $2^{-\Delta\Delta CT}$ method. Experiments were performed in triplicate and GAPDH was used as an internal control. Primers were designed by Primer Premier 6, synthesized by the Sangon Biotech Company (Shanghai, China), and listed in Table 1.

Western blot and protein stability analysis

Stably transfected HEK293T cells were seeded in six-well plates and cultured for 24 h. Total cell proteins were extracted using Radioimmunoprecipitation assay (RIPA) buffer. For the NPR2 protein stability test, stably transfected cells were treated with 20μM MG132 (MCE, USA), and whole cell proteins were collected and extracted at different time points (0, 12, 24 h) post-MG132 treatment. The BCA Protein Assay kit (Beyotime, China) was utilized to measure protein concentration. The proteins (40 μg) were separated by 7.5% sulfate-polyacrylamide gel electrophoresis (SDS-PAGE) and transferred onto polyvinylidene fluoride (PVDF) membranes (Millipore, USA). The membranes were blocked with TBS-T containing 5% non-fat milk for 1 h at room temperature, followed by overnight incubation with primary antibodies against Flag (1:1000, Sigma), actin (1:7500, ProteinTech), and GAPDH (1: 5000, Cell Signaling Technology) at 4 °C. After three washes with TBS-T, the membranes were incubated with secondary antibodies for 1 h at room temperature. Finally, the membranes were subjected to three additional washes and developed using the Super-Pico ECL chemiluminescence Kit (Vazyme, China) and Tanon 5800 Imaging System (Tanon, China).

Subcellular localization analysis of mutant NPR2 protein

Immunofluorescence and western blot determined the location of the corresponding proteins. Stably transfected HEK293T cells were seeded in six-well plates and fixed

Table 1 Primer sequences for amplifying *NPR2* and *GAPDH* gene

Target gene	Forward primer (5′-3′)	Reverse primer (5′-3′)
Human *NPR2*	ACCTCATCGCTGGCTGCTTCTA	CCCGTCCACCAAATCTGCTTCT
Human *GAPDH*	ACAACTTTGGTATCGTGGAAGG	GCCATCACGCCACAGTTTC

with 4% paraformaldehyde for 20 min. Subsequently, the cells were permeabilized with 0.5% Triton X-100 for 10 min, followed by blocking in 5% BSA (Solarbio, China) for 1 h. Immunostaining was performed using an Anti-Flag primary antibody (1:100, Proteintech, China) at 37 °C for 2 h. CoraLite594-conjugated Goat Anti-Mouse IgG (H + L) secondary antibodies (Proteintech, China) were applied at a dilution of 1:500 at room temperature for 1 h. Finally, the cells were counterstained with DAPI (Beyotime, China) to visualize the nucleus before observing protein localization using a confocal microscope (LSM800, Carl Zeiss, Germany).

The plasma membrane protein isolation kit (Beyotime, China) was employed to obtain cell membrane and cytoplasmic proteins. Protein extracts were subjected to electrophoresis and subsequent blotting as previously described. Actin (1:7500, ProteinTech) was used as an internal control for cytoplasmic proteins, while ATP1A1 (1:1000, Affinity) was used as an internal control for cell surface membrane proteins.

Enzyme-linked immunosorbent assay (ELISA)

Stably transfected HEK293T cells were seeded into 6-well plates, and incubated with 100 nM CNP (CNP-22, MCE, USA) in serum-free DMEM for 30 min at 37°C. Subsequently, the endogenous phosphodiesterase activity was inhibited by adding 0.1 M HCl to stabilize cGMP. The cGMP levels in cell lysates were measured using the cGMP Complete ELISA kit (ENZO Life Sciences, Madison Avenue, NY, USA).

Table 2 Clinical characteristic of patients with *NPR2* gene mutation

Variable	Patient 1	Patient 2
Age (years)	10.3	4.7
BA (years)	9.9	2.5
Birth length (cm)	50.0	50.0
Birth weight (kg)	3.4	3.1
Height (cm/SDS)	125.0/-2.71	97.7/-2.38
weight (kg/SDS)	25.0/-1.30	15.0/-1.23
BMI (kg/m^2)	16	15.71
Sitting height/height (ratio)	0.58	0.56
arm span /Height (ratio)	1.00	0.94
Father's height (cm/SDS)	160.0/-2.12	168.0/-1.68
Mother's height (cm/SDS)	151.0/-0.78	149.0/-2.06
Genetic target height (cm/SDS)	162.0/-1.78	165.0/-1.28
GH peak (ng/mL) [Levodopa test]	8.60	10.31
GH peak (ng/mL) [Insulin test]	8.56	-
IGF-1 (ng/mL)	25.0	117.6
IGF-1 SDS	-3.83	0.25
IGFBP-3 (μg/mL)	2.52	3.10
Final adult height (cm/SDS)	156.0/-2.78	-/-

BA, bone age; SDS, standard deviation score; BMI,body mass index; GH, growth hormone; IGF-1, insulin-like growth factor 1; IGFBP-3, insulin-like growth factor binding protein 3

Statistical analysis

The values are expressed as the mean ± standard deviation (SD). All data were analyzed using GraphPad Prism 9.0 software. Statistical analysis was performed by one-way ANOVA when more than two groups were compared. A statistical difference was considered when the *p*-value was less than 0.05.

Results

Clinical features

Patient 1, a 10.3-year-old boy, was admitted to the hospital due to short stature. On admission, his height and weight were 125.0 cm (-2.71 SDS) and 25.0 kg (-1.30 SDS), respectively, with a sitting height/height ratio of 0.58 and an arm span/ height ratio of 1.0. His bone age (BA) was 9.9 years. The patient was born at full term with a birth weight of 3.4 kg and a birth length of 50 cm. The patient's father was 160.0 cm (-2.12 SDS) and his mother was 151 cm (-1.68 SDS) in height and his genetic target height is 162.0 cm (-1.78 SDS). Additionally, the serum IGF-1 level of the patient was low (-3.83 SDS), and peak GH levels on two stimulation tests were below 10.0 ng/mL. The patient underwent recombinant human growth hormone (rhGH) for up to 5 months following the initial visit. Approximately 2 years later, he received rhGH therapy once again for up to 6 months. At the end of treatment, the patient's height was 139.9 cm (-3.08 SDS), an increase of 12.1 cm from the first visit. The patient has not received rhGH therapy since then and was followed up to adulthood, with a final height of 156.0 cm (-2.78 SDS) (Table 2).

Patient 2 was admitted to the hospital at 4.7 years old for short stature. At that time, his height was 97.7 cm (-2.38 SDS) and his weight was 15.0 kg (-1.23 SDS). He has severely delayed bone age (2.5 years). The patient was born at full-term and had a normal birth weight (3.1 kg) and birth length (50.0 cm). The patient's sitting height/height ratio is 0.56 and arm span/height ratio is 0.94. His father's and mother's height were 168.0 cm (-0.78 SDS) and 149.0 cm (-2.06 SDS), respectively. The genetic target height of the patient is 165.0 cm (-1.28 SDS). The patient's GH Peak, serum IGF-1, and IGFBP-3 levels were normal. The patient did not receive rhGH treatment and was monitored until 15 when his height was recorded as 153.0 cm (-2.58 SDS) (Table 2).

Genetic analysis

Whole exome sequencing (WES) and Sanger sequencing revealed that patient 1 carried a heterozygous nonsense mutation (c.1162 C > T, p.R388*) in the *NPR2* gene, which was inherited from the father (Fig. 1A). A heterozygous frameshift mutation of the *NPR2* gene (c.2629_2630delAG, p.S877Hfs*10) was identified in patient 2 and was inherited from the mother (Fig. 1B).

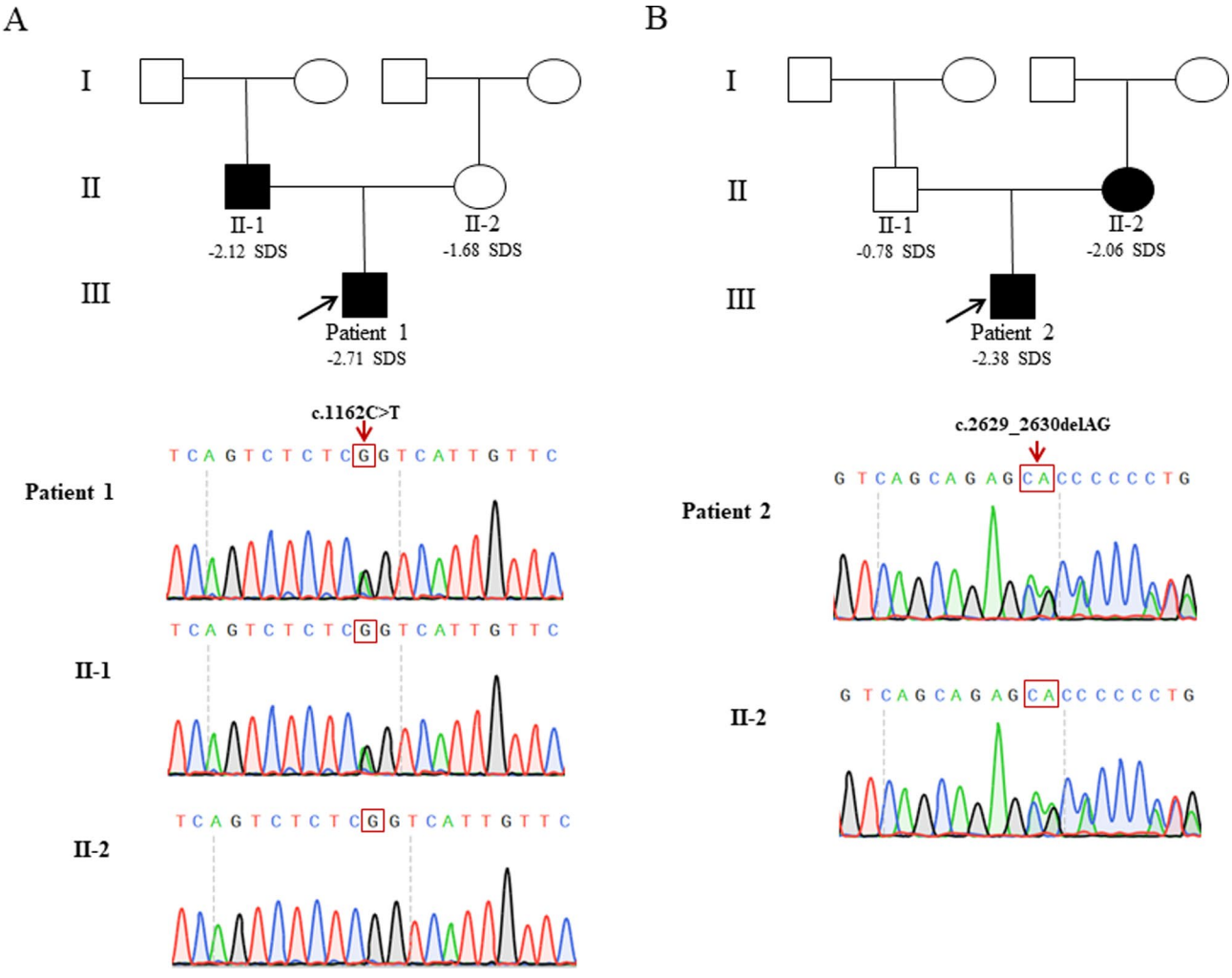

Fig. 1 Pedigree and Sanger sequencing of the patients. Pedigree and Sanger sequencing results of Patient 1 (**A**) and Patients 2 (**B**)

Both mutations result in premature termination of protein translation and form truncated NPR2 proteins, and they were referred to as truncating mutations. In addition, the p.R388* mutation has been reported to the ClinVar database (VCV000017787.9), but the p.S877Hfs*10 mutation has not been previously reported. This p.S877Hfs*10 mutation was classified as "pathogenic" (PVS1 + PM2 + PM4 + PP1 + PP4) following the ACMG/AMP guideline and has been submitted to the ClinVar database (VCV003366928.1).

Bioinformatic analysis

The two mutations, p.R388* and p.S877Hfs*10, occur in the ligand-binding domain (ECD) and guanylyl cyclase (GC) domains of the NPR2 protein, respectively (Fig. 2A). Conservation analysis showed that the target amino acid for mutation is highly conserved among different species (Fig. 2B). Three-dimensional (3D) structure prediction of the wild-type (WT) and mutant NPR2 proteins using Alphafold and Pymol software, revealed that the NPR2 mutant proteins were truncated with an altered spatial conformation (Fig. 2C, D).

Expression and protein stability of wild type (WT) and mutant NPR2 proteins

The qRT-PCR results revealed a significant increase in mRNA levels of mutant NPR2 compared to the WT (Fig. 3A). The Western blot analysis showed that the WT NPR2 protein band was approximately 115 kD, whereas two mutations (p.R388* and p.S877Hfs*10) produced two truncated NPR2 protein bands at approximately 43 kD and 98 kD, respectively. Notably, the expression of the truncated NPR2 proteins was significantly lower than that of the WT (Fig. 3B).

The high transcript levels and low protein expression suggest that both mutant proteins may be degraded in HEK293T cells. To study further, the stability of both WT and mutant NPR2 proteins were investigate using MG132. MG132 is an inhibitor of the proteasome and was used to inhibit protein degradation. After 12 h of

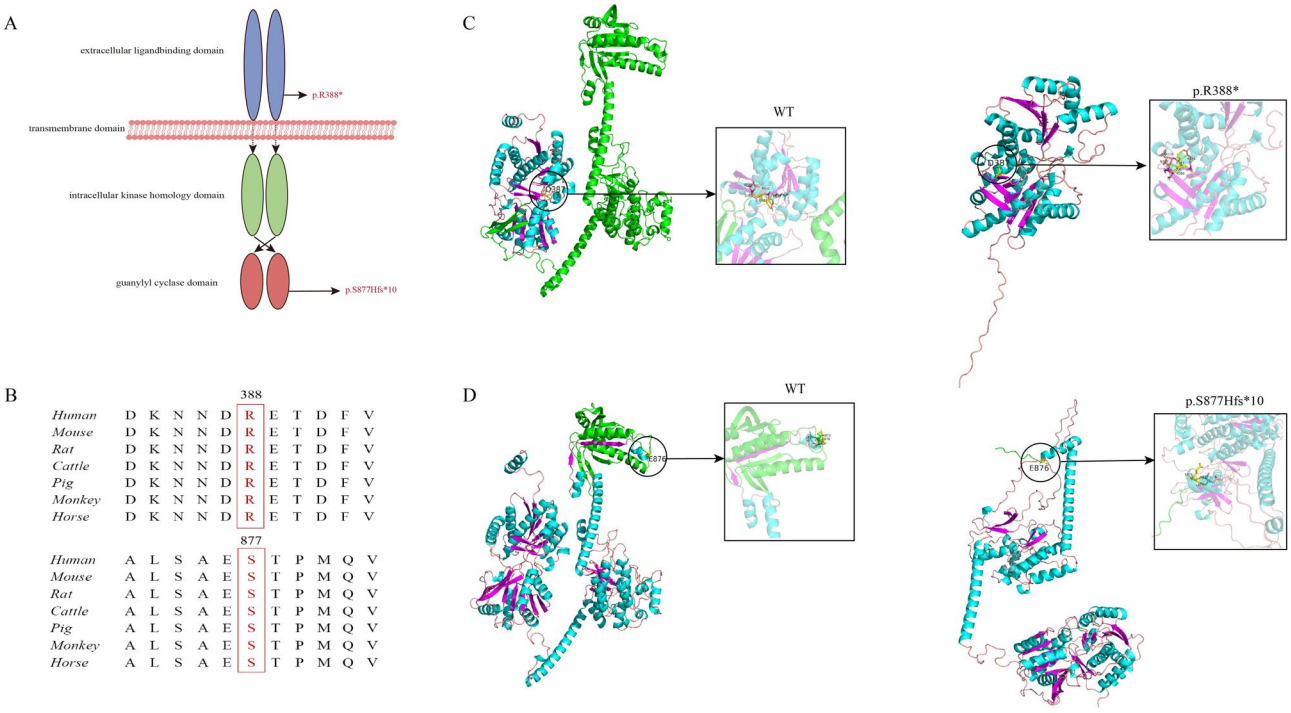

Fig. 2 Bioinformatics analysis was conducted on two NPR2 mutations. (**A**) The schematic diagram illustrates the domain structure of the NPR2 protein and the locations of two mutations. (**B**) A conservative analysis was performed on amino acid residues in the NPR2 protein across different species, highlighting the 388th and 877th amino acids R (arginine) and S (serine) in red. (**C**, **D**) Alphafold and Pymol software were used to predict the 3D structures of both WT and mutant (p.R388* & p.S877Hfs*10) NPR2 proteins. Arrows on the protein illustration indicate positions of affected amino acid residues in NPR2 proteins. 3D: three-dimensional, WT: wild type

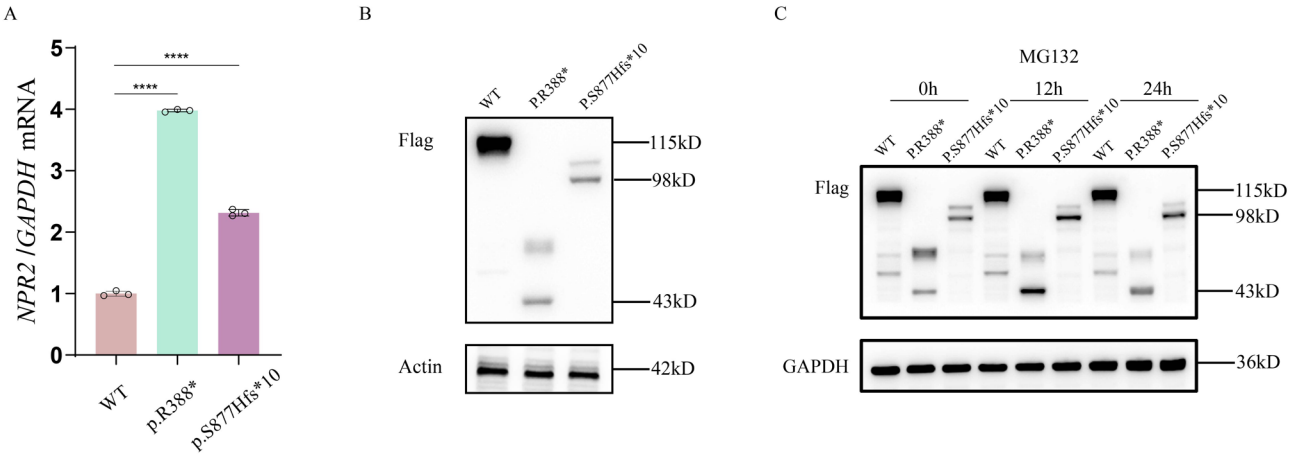

Fig. 3 Impact of *NPR2* mutations (p.R388* and p.S877Hfs*10) on their expression and stability in HEK293T cells. (**A**) Relative quantitative analysis of mRNA levels of WT and mutant NPR2 by qRT-PCR.; (**B**) Expression of WT and mutant NPR2 proteins by Western blot; (**C**) The impact of MG132 treatment for different durations on the stability of NPR2 protein was assessed by Western blot. WT: wild type; h: hour/hours; ****$p < 0.0001$

MG132 treatment, we observed that the level of WT NPR2 protein remained unchanged, whereas the level of mutant NPR2 protein increased (Fig. 3C). These findings indicate reduced stability and increased degradation of the truncated NPR2 proteins.

Subcellular localization of wild-type (WT) and mutant NPR2

Immunofluorescence analysis revealed that the WT NPR2 protein displayed a dense distribution on the cell surface with well-defined cell boundaries. In contrast, mutant NPR2 proteins were predominantly localized in the cytoplasm rather than on the cell membrane (Fig. 4A). To further confirm the subcellular localization

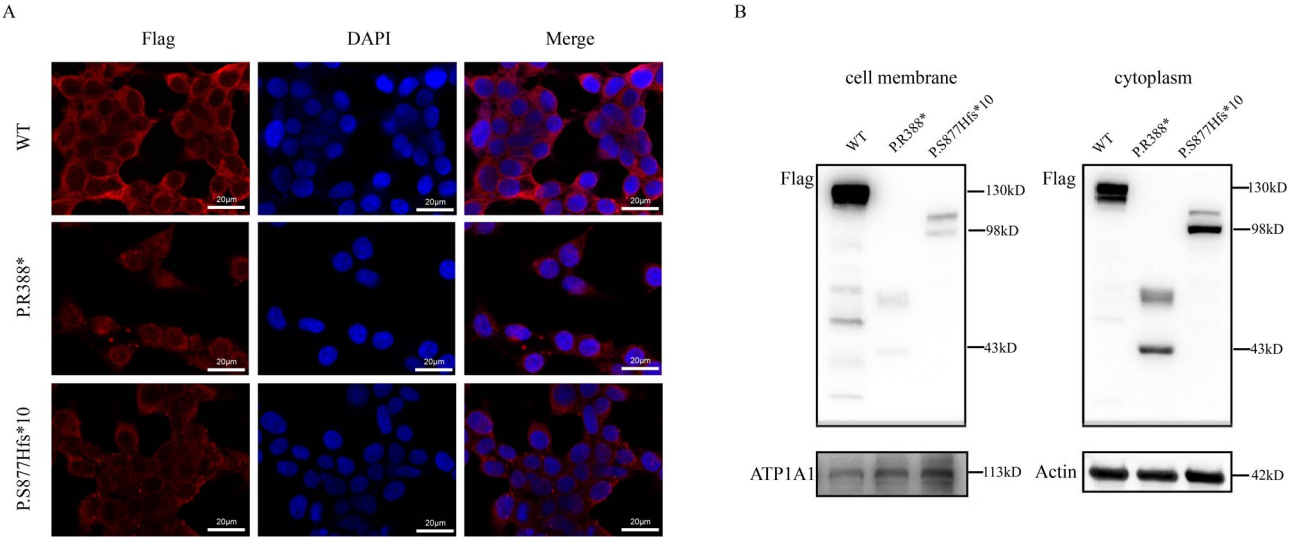

Fig. 4 Impact of *NPR2* mutations (p.R388* and p.S877Hfs*10) on their subcellular localization in HEK293T cells. (**A**) Subcellular distribution of NPR2 protein (red) by immunofluorescence analysis, with DAPI staining the cell nucleus. Scale bar: 20 μm. (**B**) The NPR2 protein expression distribution in the cell membrane and cytoplasm was assessed by Western blot

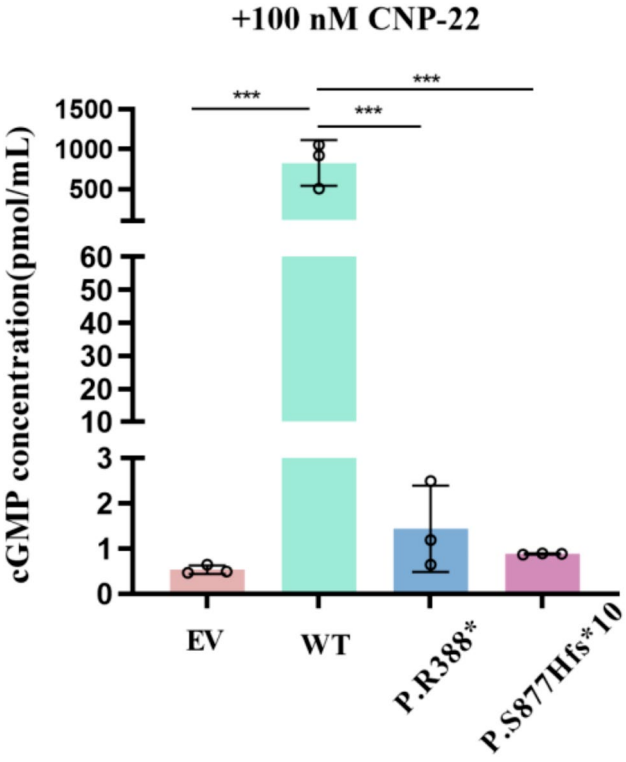

Fig. 5 Impact of NPR2 mutations (p.R388* and p.S877Hfs*10) on its ability to stimulate cyclic guanosine monophosphate (cGMP) production in the HEK293T cells. The cGMP production in cells overexpressing NPR2 (wild type or mutants) was measured following C-type natriuretic peptide-22 (CNP-22) stimulation using Enzyme-Linked Immunosorbent Assay (ELISA). WT: wild type. EV: empty vector. $^{**}p < 0.01$, $^{***}p < 0.001$

of mutant NPR2 proteins, distinct fractions of the cell membrane and cytoplasmic proteins were isolated and subjected to western blot analysis. The results indicated that mutant NPR2 proteins were detected primarily in the cytoplasmic fraction and minimally in the cell membrane fraction (Fig. 4B). These findings indicate that the p.R388* and p.S877Hfs*10 mutations result in impaired localization of the NPR2 protein to the cell membrane.

Functional analysis of wild-type (WT) and mutant NPR2

To evaluate the impact of mutations on NPR2 protein function, we measured cGMP levels in HEK293T cells after 100nM CNP-22 stimulation. The production of cGMP was significantly lower in cells expressing mutant NPR2 compared to those expressing WT NPR2 (Fig. 5). These findings indicate that both p.R388* and p.S877Hfs*10 mutations result in a greatly reduced function for NPR2 proteins in generating cGMP upon CNP stimulation.

Discussion

In the present study, we identified two *NPR2* truncating mutations (c.1162 C > T, p.R388* and c.2629_2630delAG, p.S877Hfs*10) in two Chinese boys that co-segregated with short stature in the family. Our cellular assays revealed that the truncating mutations escaped nonsense-mediated mRNA decay (NMD), producing a truncated protein but with reduced stability. Furthermore, the truncated NPR2 protein exhibited abnormal intracellular localization, and could not be transferred to the cell membrane, resulting in a significant diminution of signal transduction functionality. These findings contribute valuable insights into the pathogenic mechanism

underlying short stature resulting from *NPR2* truncating mutations.

A multitude of genes play critical roles in modulating signaling pathways associated with bone growth. the *WFS1* genes is involved in the growth hormone signaling pathway [19, 20], *PTPN11* is associated with essential cellular processes signaling pathways, *ACAN* participates in the cartilage extracellular matrix signaling pathway, and *NPR2* is implicated in paracrine signaling pathways [6]. As a key gene in the paracrine signaling pathway, NPR2 regulates skeletal growth by stimulating cyclic guanosine monophosphate (cGMP) production upon binding to its ligand (CNP) [21]. This study identified two truncating mutations in the *NPR2* gene, inherited from the father and the mother, respectively. The p.R388* mutation may cause the NPR2 polypeptide to terminate at the codon 388 amino acid, causing truncated protein to form. Another mutation, p.S877Hfs*10, causes an amino acid substitution at position 877 (p.S877H) followed by 10 new amino acids before a stop codon occurs to terminate the NPR2 protein prematurely. Both mutations were detected by WES confirmed by Sanger sequencing. WES offers a dependable and cost-effective approach for identifying mutations within the exon regions of genes [22]. However, when comprehensive genomic information from noncoding regions is required, whole genome sequencing (WGS) becomes necessary. WGS boasts a broader detection spectrum, enabling the identification of mutations in both coding and noncoding regions, thereby detecting a greater number of genes compared to WES [23].

Bioinformatics approaches were performed to predict the potential impacts of these two mutations on the structure and function of the NPR2 protein. Both mutations affect amino acids that are highly conserved across different species, indicating that the mutations of those amino acids have more significant impacts on the structure and function of the NPR2 protein [24]. The p.R388* mutation was located in the extracellular ligand-binding domain (ECD) of the NPR2 protein, not only potentially influencing its binding to the receptor CNP but also resulting in the deletion of the remaining three domains (the transmembrane domain, the KHD, and the GC domain). We hypothesize that CNP hardly stimulates this mutant NPR2 to generate cGMP. Another mutation, p.S877Hfs*10, emerges in the GC domain, undermining the integrity of this crucial domain and guanylate cyclase activity. This mutation might confer normal binding affinity with CNP, yet will severely impact cGMP production [25].

In this study, the pathogenicity and pathogenesis of the two truncating mutations were investigated in HEK293T cells. Both mutations lead to premature termination of the mRNA sequences, resulting in the production of truncated proteins. Normally, prematurely terminated mRNAs are subject to degradation by nonsense-mediated decay (NMD) [26]. This study found that both mutations can evade the NMD mechanism and synthesize truncated NPR2 proteins, but the expression level of truncated proteins is lower than that of WT NPR2. This result is inconsistent with a previous result obtained from Mustafa et al. [27]. They reported a nonsense mutation (c.613 C > T, p.R205X) of the *NPR2* gene that generated a truncated NPR2 protein (25kD) showing higher expression as compared to WT NPR2. This suggests that truncating mutations in the ECD of NPR2 may exert diverse impacts on protein expression. Moreover, the ability of the two truncated NPR2 proteins to stimulate cGMP production was greatly reduced, which was similar to the truncated mutation (p.H948Pfs*5, p.H840*) studied by Chen et al. [28]. Our study further demonstrated that the stability of the truncated protein was poor, which may explain the mechanism of the loss-of-function truncating mutations in NPR2.

In addition, several previous studies [13, 29–32] have revealed that approximately 58% (15/26) of *NPR2* missense mutations impact the protein's normal transport to the cell membrane independent of the mutation position. However, much less NPR2 truncated protein subcellular localization analysis has been carried out. Li and others [13] reported that both truncating mutations of *NPR2* result in the failure of protein localization on the cell membrane and retention in the cytoplasm, leading to the loss of function of the mutant protein, which is consistent with our findings. Therefore, defective cellular trafficking to the cell membrane is likely a major molecular mechanism of the truncating *NPR2* mutations. Protein folding in the endoplasmic reticulum (ER) is monitored by ER quality control mechanisms, and misfolding proteins are retained and degraded in the ER by an ER-associated degradation pathway [33]. We speculate that a change in conformation of the truncated NPR2 receptor promotes protein misfolding and degradation in the ER, and defects in the normal intracellular trafficking from the ER to the cell membrane.

Heterozygous mutations in *NPR2* could be an important cause of short stature and may be associated with diverse phenotypes [31, 34]. A previous study reported 46 patients with *NPR2* heterozygous mutations all presented with short stature, half with skeletal deformities, and 1/5 with facial abnormalities [35]. However, another study reported two patients carrying heterozygous missense mutations in the *NPR2* gene who showed only a short stature and no other skeletal dysplasia [36]. In addition, two patients with *NPR2* truncating mutations in this study exhibited short stature without other notable deformities or skeletal abnormalities. Therefore, the relationship between the genotype and phenotype of patients

with *NPR2* heterozygous mutations is still unclear, and more cases are needed to determine whether the complexity of the phenotype is related to the mutation type or mutation location. Patients carrying heterozygous *NPR2* mutations display a progressive decline of age-adjusted height z -scores eventually leading to severe short stature [37], suggesting that short stature due to *NPR2* mutations should be treated early. Recombinant human growth hormone (rhGH) appears beneficial in treating short stature due to *NPR2* gene heterozygous mutations [38]. However, there are significant differences in response to rhGH treatment between patients, which may be related to the location of the mutation, such as patients with mutations in the ECD of NPR2 typically respond poorly to rhGH [35]. In this study, patient 1 showed a poor respond to rhGH treatment and the height changed from 125.0 cm (-2.71SDS) to 139.9 cm (-3.08SDS) after treatment. This might be associated with poor continuity of rhGH treatment and the fact that the mutation in this patient emerged in the ECD of NPR2. Unfortunately, patient 2 in this study was not treated with rhGH and remains short at -2.58 SDS of height when reaching the age of 15 years. Therefore, the efficacy of rhGH treatment in patients with *NPR2* heterozygous mutations still needs to be investigated in a larger population with long-term follow-up.

There were some limitations to our study. First, our results demonstrate that both of these truncating mutations affect the subcellular localization and stability of NPR2. However, the specific mechanism is unclear and further research is needed. Second, patient 2 exhibited a mutation within the GC domain of the NPR2 protein and did not receive rhGH therapy. Consequently, it was not possible to assess the impact of rhGH treatment on GC domain mutations.

In conclusion, our study has identified two truncating mutations in the *NPR2* gene in two Chinese families with short stature. The two mutations could potentially impact the expression, subcellular localization, stability, and function of NPR2 proteins. These findings not only expand the mutational spectrum of the *NPR2* gene but also provide new insights into the pathogenesis of short stature resulting from heterozygous *NPR2* truncating mutations.

Abbreviations

CNP	C-type natriuretic peptide
NPR2	Natriuretic peptide receptor 2
cGMP	cyclic guanosine monophosphate
ECD	Extracellular ligand-binding domain
KHD	Kinase homology domain
GC	Guanylyl cyclase
AMDM	Acromesomelic dysplasia Maroteaux type
WES	Whole-Exome Sequencing
NMD	Nonsense-mediated mRNA Decay
BMI	Body Mass Index
GH	Growth hormone
IGF-1	Insulin-like Growth Factor-1
IGFBP-3	Insulin-like Growth Factor Binding Protein-3
BA	Bone age
GP	Greulich-Pyle
ACMG-AMP	American College of Medical Genetics and Genomics and Association for Molecular Pathology
AI	Adobe Illustrator
3D	Three-Dimensional
EV	Empty vector
GFP	Green fluorescent protein
qPCR	quantitative real-time PCR
RIPA	Radioimmunoprecipitation assay
SDS	Standard Deviation Score
ELISA	Enzyme-Linked Immunosorbent Assay
WT	Wild type
ER	Endoplasmic reticulum

Supplementary Information

The online version contains supplementary material available at https://doi.org/10.1186/s12887-025-05478-y.

Supplementary Material 1

Acknowledgements

We are grateful to the patients and their parents for participating in this study.

Author contributions

SSW drafted the first versions of the manuscript. BB and QQZ were responsible for the design of the project and revised the manuscript. RL, MZ and YYL made the clinical evaluation and collected clinical information of the patients in detail. CPZ and FPL provided software support. SSW, DYH, SXC and FPL performed the experiments and data analysis.All authors reviewed the manuscript.

Funding

This study was supported by the Natural Science Foundation of Shandong Province (No. ZR2022MH284).

Data availability

No datasets were generated or analysed during the current study.

Declarations

Ethics approval and consent to participate

The study was approved by the Affiliated Hospital of Economics and Medical Sciences Ethics Committee. Written informed consent was obtained from the patient's parents for publication.

Consent for publication

Not applicable.

Competing interests

The authors declare no competing interests.

Received: 15 October 2024 / Accepted: 31 January 2025
Published online: 24 February 2025

References

1. Jee YH, et al. Genetics of short stature. Endocrinol Metab Clin North Am. 2017;46(2):259–81.
2. Lui JC, Nilsson O, Baron J. Recent research on the growth plate: recent insights into the regulation of the growth plate. J Mol Endocrinol. 2014;53(1):T1–9.
3. Wit JM, et al. MECHANISMS IN ENDOCRINOLOGY: novel genetic causes of short stature. Eur J Endocrinol. 2016;174(4):R145–73.
4. Li X, et al. Clinical profiles and genetic Spectra of 814 Chinese children with short stature. J Clin Endocrinol Metab. 2022;107(4):972–85.

5. Fan X, et al. Exome sequencing reveals genetic architecture in patients with isolated or syndromic short stature. J Genet Genomics. 2021;48(5):396–402.
6. Zhao Q, et al. Molecular diagnosis is an important indicator for response to growth hormone therapy in children with short stature. Clin Chim Acta. 2024;554:117779.
7. Vasques GA, Arnhold IJ, Jorge AA. Role of the natriuretic peptide system in normal growth and growth disorders. Horm Res Paediatr. 2014;82(4):222–9.
8. Langenickel T, et al. Forced homodimerization by site-directed mutagenesis alters guanylyl cyclase activity of natriuretic peptide receptor B. Hypertension. 2004;43(2):460–5.
9. Wu J, et al. Novel loss-of-function mutations in NPR2 cause Acromesomelic Dysplasia, Maroteaux Type. Front Genet. 2022;13:823861.
10. Tsuji T, Kunieda T. A loss-of-function mutation in natriuretic peptide receptor 2 (Npr2) gene is responsible for disproportionate dwarfism in cn/cn mouse. J Biol Chem. 2005;280(14):14288–92.
11. Bartels CF, et al. Mutations in the transmembrane natriuretic peptide receptor NPR-B impair skeletal growth and cause acromesomelic dysplasia, type Maroteaux. Am J Hum Genet. 2004;75(1):27–34.
12. Hanley PC, et al. Short stature is progressive in patients with heterozygous NPR2 mutations. J Clin Endocrinol Metab. 2020;105(10):3190–202.
13. Li Q et al. Novel NPR2 gene mutations affect chondrocytes function via ER stress in short stature. Cells. 2022;11(8).
14. Li H, et al. [Height and weight standardized growth charts for Chinese children and adolescents aged 0 to 18 years]. Zhonghua Er Ke Za Zhi. 2009;47(7):487–92.
15. Boogers LS, et al. Transgender girls Grow Tall: adult height is unaffected by GnRH Analogue and Estradiol Treatment. J Clin Endocrinol Metab. 2022;107(9):e3805–15.
16. Cao B, et al. Pediatric continuous reference intervals of serum insulin-like growth factor 1 levels in a Healthy Chinese Children Population - based on PRINCE Study. Endocr Pract. 2022;28(7):696–702.
17. Hojreh A, et al. Hand MRI and the Greulich-Pyle atlas in skeletal age estimation in adolescents. Skeletal Radiol. 2018;47(7):963–71.
18. Richards S, et al. Standards and guidelines for the interpretation of sequence variants: a joint consensus recommendation of the American College of Medical Genetics and Genomics and the Association for Molecular Pathology. Genet Med. 2015;17(5):405–24.
19. Kõks S, et al. Wfs1 gene deletion causes growth retardation in mice and interferes with the growth hormone pathway. Physiol Genomics. 2009;37(3):249–59.
20. Kõks S. Genomics of Wolfram Syndrome 1 (WFS1). Biomolecules. 2023;13(9).
21. Brown KM, Sibley LD. Essential cGMP signaling in Toxoplasma is initiated by a hybrid P-Type ATPase-Guanylate cyclase. Cell Host Microbe. 2018;24(6):804–e8166.
22. Lönnstedt IM, et al. Deciphering clonality in aneuploid breast tumors using SNP array and sequencing data. Genome Biol. 2014;15(9):470.
23. Adams DR, Eng CM. Next-generation sequencing to Diagnose Suspected Genetic disorders. N Engl J Med. 2018;379(14):1353–62.
24. Hirata H, et al. ZC4H2 mutations are associated with arthrogryposis multiplex congenita and intellectual disability through impairment of central and peripheral synaptic plasticity. Am J Hum Genet. 2013;92(5):681–95.
25. Hachiya R, et al. Intact kinase homology domain of natriuretic peptide receptor-B is essential for skeletal development. J Clin Endocrinol Metab. 2007;92(10):4009–14.
26. Hu W, et al. Nonsense-mediated mRNA decapping occurs on polyribosomes in Saccharomyces cerevisiae. Nat Struct Mol Biol. 2010;17(2):244–7.
27. Mustafa S, et al. A novel nonsense mutation in NPR2 gene causing Acromesomelic dysplasia, type Maroteaux in a consanguineous family in Southern Punjab (Pakistan). Genes Genomics. 2020;42(8):847–54.
28. Chen H, et al. Novel pathogenic NPR2 variants in short stature patients and the therapeutic response to rhGH. Orphanet J Rare Dis. 2023;18(1):221.
29. Hisado-Oliva A, et al. Heterozygous NPR2 mutations cause disproportionate short stature, similar to Léri-Weill Dyschondrosteosis. J Clin Endocrinol Metab. 2015;100(8):E1133–42.
30. Badawi S, et al. Unveiling the pathogenic mechanisms of NPR2 missense variants: insights into the genotype-associated severity in acromesomelic dysplasia and short stature. Front Cell Dev Biol. 2023;11:1294748.
31. Vasques GA, et al. Heterozygous mutations in natriuretic peptide receptor-B (NPR2) gene as a cause of short stature in patients initially classified as idiopathic short stature. J Clin Endocrinol Metab. 2013;98(10):E1636–44.
32. Amano N, et al. Identification and functional characterization of two novel NPR2 mutations in Japanese patients with short stature. J Clin Endocrinol Metab. 2014;99(4):E713–8.
33. Hume AN, et al. Defective cellular trafficking of missense NPR-B mutants is the major mechanism underlying acromesomelic dysplasia-type Maroteaux. Hum Mol Genet. 2009;18(2):267–77.
34. Estrada K, et al. Identifying therapeutic drug targets using bidirectional effect genes. Nat Commun. 2021;12(1):2224.
35. Ke X, et al. Clinical characteristics of short-stature patients with an NPR2 mutation and the therapeutic response to rhGH. J Clin Endocrinol Metab. 2021;106(2):431–41.
36. Hwang IT, et al. Role of NPR2 mutation in idiopathic short stature: identification of two novel mutations. Mol Genet Genomic Med. 2020;8(3):e1146.
37. Kanai Y, et al. Circulating osteocrin stimulates bone growth by limiting C-type natriuretic peptide clearance. J Clin Invest. 2017;127(11):4136–47.
38. Plachy L et al. NPR2 variants are frequent among children with familiar short stature and respond well to growth hormone therapy. J Clin Endocrinol Metab. 2020;105(3).

Publisher's note